Behavioral models of microwave circuits with fading memory.

Nicholas B. Tufillaro
Agilent Technologies, 3500 Deer Creek Road, MS 24M-A, Palo Alto, CA 94303-0867

David M. Walker
Center for Applied Dynamics and Optimization, The University of Western Australia, Nedlands, Perth, WA 6907, Australia
(October 16, 2000)

We discuss how to build nonlinear input-output models of low-dimensional deterministic systems for both static and dynamic (feedback) systems with "fading memory." Radial basis functions are used to build the models. The utility of these models is illustrated by building accurate and stable models for electronic circuits with dynamic (memory) effects.

We are developing techniques for building black-box models for a number of simple electronic components (e.g. transistors) and circuits (e.g. amplifiers) [1-12]. An example of a such a circuit we built a model for is shown in Fig. 1.

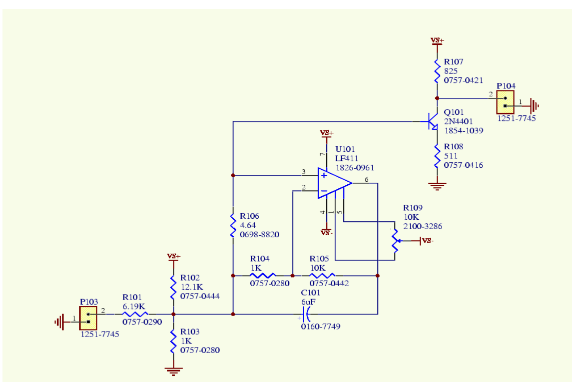

FIG. 1. A high frequency "analog" transistor circuit.

This particular circuit is meant to be a transistor 'analog' of a high-frequency microwave transistor [13]. In addition to acting as an amplifier, this circuit also tries to mimic certain (memory dependent) charge storage effects which should be active in this example in a frequency range around 0.5 kHz. Models are also built from numerical models and data from simulations.

The notion of a system having "fading memory" is that input signals far in the past should have almost no effect on the present state. A precise mathematical definition of this concept is usually stated in the space of input/output functional (integral) equations. Boyd and Chua hint that the notion of fading memory should also have a (differential) state space formulation [4]. In the following example, we show that the essential ingredients of such a state space formulation is that the attracting solution should forget both its initial condition and input sequences far in the past. Both conditions are usually fulfilled if the system has a unique attracting fixed point.

Consider a closed RC circuit driven by a voltage source v_s. The voltage around a closed loop is

$$v_s - V_C - V_R = v_s - \frac{1}{C}\int_0^t i dt - Ri = 0 \qquad (1)$$

or, differentiating with respect to time,

$$\frac{di}{dt} + \frac{1}{RC} i = \frac{1}{R}\frac{dv_s}{dt}. \qquad (2)$$

The voltage source is triangular wave form defined as follows. For an integer n and a real time

$$\tau = t_{n+1} - t_n, \qquad (3)$$

v_s is a linear function of the voltage with slope plus or minus one. The slope's sign randomly changes sign at each instant indexed by n. The waveform is thus a random walk. By construction,

$$\frac{dv_s}{dt} = s_n, \quad s_n \in \{-1, +1\} \qquad (4)$$

generates a random sequence of form

$$\{\ldots, +1, +1, -1, +1, -1, -1, -1, +1, \ldots\}.$$

The equation of motion for the current is then

$$\frac{di}{dt} = \frac{-1}{RC} i + \frac{1}{R} s_n. \qquad (5)$$

Depending of the sign s_n, the equation contains two possible equilibrium points ($di_*/dt = 0$),

$$i_* = C s_n, \quad s_n \in \{-1, +1\}. \qquad (6)$$

When $t \neq t_n$, $n = 0, 1, 2, \ldots$, the equation of motion is easy to solve by considering the motion relative to the equilibrium point,

$$y = i - C s_n, \qquad (7)$$

then

$$\frac{dy}{dt} = \frac{-1}{RC} y \qquad (8)$$

with solution

$$y(t) = y_0 e^{-\frac{1}{RC} t}. \qquad (9)$$

Next the current is found in the original coordinates at each t_{n+1} $(i(n\tau) = i_n)$,

$$i_{n+1} = e^{-\frac{1}{RC}\tau} i_n + C(1 - e^{-\frac{1}{RC}\tau}) s_n. \tag{10}$$

Now to make the example as simple as possible, set

$$e^{-\frac{1}{RC}\tau} = \frac{1}{3}. \tag{11}$$

which implies

$$i_{n+1} = \frac{1}{3} i_n + \frac{2}{3} C s_n, \quad s_n \in \{-1, +1\}. \tag{12}$$

Lastly, we can solve for i_{n+1} in terms of past values of the drive voltage and initial condition. First, rescale the current by C $(j = Ci)$,

$$j_{n+1} = \frac{1}{3} j_n + \frac{2}{3} s_n. \tag{13}$$

Next solve for j_{n+1} in terms of m iterations in the past $(d = 0, 1, 2, ...)$,

$$j_{n+1} = \frac{1}{3^{m+1}} j_{n-m} + \frac{2}{3} \sum_{d=0}^{m} \frac{1}{3^d} s_{n-d}. \tag{14}$$

Note that the sum in the series is a geometric series so the sum is dominated by the first few terms. Fading memory is easy to see in this result. For large memory depth, m, the current value of j_{n+1} has little dependence on j_{n-m} and the higher order terms in $\sum_{d=0}^{m} \frac{1}{3^d} s_{n-d}$.

Returning to our experimental example, for the experimental data, voltage excitations are supplied and their amplified response are measured using a nonlinear circuit measurement system. The measurement system combines nonlinear circuit device models, arbitrary wave form generation cards, analog-to-digital cards and numerical software package all developed in, and controlled by, Matlab [14]. We can thus generate time domain input-output (stimuli-response) data for nonlinear circuit devices either in measurements or simulations. The particular example we use in this study is the high frequency amplifier analog in Fig. 1 with the resonance frequency set to 650Hz. The drive signals we use as stimuli are a type of CDMA like signal as well as periodic drive signals for some additional tests. The data sets are labelled by the type of signal and the carrier frequency. Thus C_{500} refers to a CDMA signal with carrier frequency 500Hz. We generate numerous data sets of different types with frequencies at 50Hz intervals starting at 50Hz and ending at 1200Hz. Voltage samples are equally spaced with a sampling frequency usually about (1/64)th of the center frequency.

This is greatly oversampled because memory constraints are not a consideration. As described below, we typically decimate the data sets and use only a fraction of them in building models. The number of points used to build a given model is usually less than 20,000 points, and can be as little as 2000.

The circuits behavior is described by embedding both the inputs and outputs in the form

$$\begin{aligned} z(t) = F[&y(t-\tau), y(t-2\tau), ..., y(t-l\tau), \\ &u(t), u(t-\tau), ..., u(t-(k-1)\tau)] \end{aligned} \tag{15}$$

where F is fitted to the data using nonlinear modeling methods such polynomials or neural nets. The models we built in this example used an embedding of the following form:

$$y(t+1) = F\big[y(t-1), y(t), u(t), u(t+1)\big]. \tag{16}$$

We found that the best models could be build by decimating the data to have approximately 12 to 16 points per cycle, and then we reconstruct models of the form of Eq. 16 with this decimated data. For example for the data set C_{1200} we have approximately 48 points per cycle. We create four data sets by decimating the original data by four, i.e., we take every fourth point. So, when we reconstruct a model of the form of Eq. 16 we are essentially reconstructing a feedback model of the form

$$y(t+4) = F\big[y(t-4), y(t), u(t), u(t+4)\big]. \tag{17}$$

We approximate the output with "static" radial basis functions of the form,

$$y(t+1) = \beta + \alpha \cdot z(t) + \sum_{i=1}^{M} \omega_i \phi(\|c_i - z(t)\|), \tag{18}$$

where z has no dependence on y, and "dynamic" radial basis models,

$$\phi(\|\mathbf{c} - z\|) = e^{-\frac{1}{2v^2}\|c-y\|^2} \big[e^{-\frac{1}{2w^2}\|d\|^2} - e^{-\frac{1}{2w^2}\|d-u\|^2}\big] \tag{19}$$

where β, α and ω are constant parameters to be estimated, and in the dynamic models y represents the part of z reconstructed using the outputs, and u represents the parts of z reconstructed from the inputs. The c are the "output" centers with the same dimension of y, and similarly the d are the "input" centers with the same dimension as u. The models which are "dynamic" have feedback; past predicted values of the output are used in the current prediction of the output. Such models are typically unstable, however, the use of a fading memory assumption in the construction of equation Eq. 19 often results in stable solutions. More details of this particular model form are presented in references [15,16].

We present the results of modeling and simulating the CDMA data sets with static and dynamic models in Table I. Table I has seven columns. The first column indicates the data set and the second column indicates the decimation used. The third column shows the "size" of our best reconstructed feedback model, i.e., the number of model coefficients. In column four we give a percentage error of the feedback model for out-of-sample drive signals and express this error in terms of signal-to-noise in column five. We calculate the signal-to-noise ratio using

$$\mathrm{SNR} = 20 \log_{10} \left(\frac{\mathrm{std}(actual)}{\mathrm{std}(errors)} \right) \mathrm{dB}. \tag{20}$$

We show the analogous results obtained by reconstructing and testing static models on the same data in the remaining columns.

Data	Dec	#Parms	RMS/std(y)	SNR	#Parms	SNR
C_{100}	1	21	0.06	25.06	7	20.76
C_{200}	1	16	0.05	26.22	3	11.77
C_{300}	1	14	0.06	24.75	7	7.58
C_{400}	1	15	0.08	21.64	5	3.24
C_{500}	1	24	0.09	21.13	3	1.71
C_{600}	2	26	0.09	21.08	3	2.15
C_{700}	3	29	0.06	23.33	2	1.85
C_{800}	3	29	0.08	21.77	2	1.43
C_{900}	4	34	0.08	21.94	3	1.80
C_{1000}	4	36	0.1046	19.60	2	1.01
C_{1100}	4	41	0.1077	19.36	2	0.75
C_{1200}	4	33	0.12	18.78	2	0.66

TABLE I. Results of simulating reconstructed feedback vs static models. Dec (decimation). Dynamic models, columns 3, 4 and 5. Static models, columns 6 and 7.

Typical results are presented in Figure 2a–d where we show sections of the time series produced by simulating the models compared to the actual measured values of the device. We show the results obtained by simulating the models reconstructed using the C_{300}, C_{600}, C_{900}, and C_{1200} data sets. Good agreement is seen in the Figures as expected from the numbers given in Table I. These simulations are also superior to the results we obtained using the best static models we could reconstruct. In most of the cases examined the long-term solutions are not sensitive to the initial seed value and, in the case of periodic drives, they appear to converge to a unique solution.

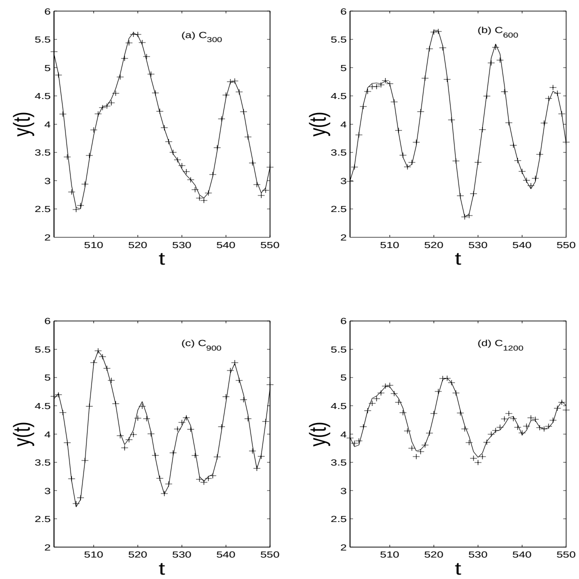

FIG. 2. Sections of feedback simulations for data sets (a) C_{300}, (b) C_{600}, (c) C_{900} and (d) C_{1200}. The solid lines are the actual device response and the crosses are the simulated predictions.

We have shown how to construct stable, free running, input-output models for a class of electronic devices and circuits having fading memory and (in the absence of a drive signal) converge to a constant solution. The models are built from band-limited, spread spectrum excitations, and such excitations provide a sufficiently rich training set to make accurate predictions of periodic or similar spread spectrum drive signals.

Acknowledgments

We thank Reggie Brown for some early discussions about this investigation and Paul Gross with assistance in building the circuit. The National Science Foundation partially supported this work through the grant NSF #9724707.

[1] H. Kantz and T. Schrieber, Nonlinear time series analysis (Cambridge, 1997); H. Abarbanel, R. Brown, J. Sidorowich, and L. Tsimring, *The analysis of observed chaotic data in physical systems*, Rev. Mod. Phys. **65**, 1331-1392 (1993).

[2] N. Tufillaro, D. Usikov, L. Barford, D. Walker, and D. Schreurs, *Measurement driven models of nonlinear electronic components*. 54th ARFTG Conference Digest, Boston, MA (USA), June 2000; Alistair I. Mees, Michael F. Jackson, and Leon O. Chua. Device modeling by radial basis functions. IEEE Trans CAS/FTA, **39**(1):19–27, 1992.

[3] L. Chua, C. Desoer, and E. Kuh, Linear and Nonlinear Circuits, (McGraw-Hill, San Francisco, 1987).

[4] S. Boyd and L. Chua, *Fading memory and the problem of approximating nonlinear operators with Volterra series*, IEEE Trans. Circ. and Sys. **CAS-32** (11), 1150-1161 (1985).

[5] Neil A. Gershenfeld, The Nature of Mathematical Modeling (Cambridge University Press, 1999).

[6] M. Casdagli, *A dynamical systems approach to modeling input-output systems*, in Nonlinear Modeling and Forecasting, SFI Studies in the Sciences of Complexity, Proc. Vol XII, Eds. M. Casdagli and S. Eubank, Addison-Wesley, 1992.

[7] S. Haykin and J. Principe, *Making sense of a complex world*, IEEE Signal Processing Magazine, 66-81 (May 1998).

[8] J. Stark, *Delay Embeddings of Forced Systems: I Deterministic Forcing,* J. Nonlinear Science, **9** 255-332, 1999; J. Stark, D.S. Broomhead, M.E. Davies and J. Huke, Delay Embeddings of Forced Systems: II Stochastic Forcing (preprint); F. Takens, *Detecting strange attractors in turbulence*, p. 366-381 of: D. Rand and L. Young (eds), Dynamical Systems and Turbluence, Lecture Notes in Mathematics, vol. **898**. New York, NY, Springer-Verlag 1981.

[9] G. F. Franklin, Feedback control of dynamic systems (Addison-Wesley, 1994.)

[10] David M. Walker and Nicholas B. Tufillaro, *Phase space reconstruction using input-output time series data,* Phys. Rev. E **60** (4), 4008-4013, 1999; C. Rhodes and M. Morari, *Determining the model order of nonlinear input–output systems*, Proceedings of the American Control Conference, Seattle, 2190–2195, 1995; L. Cao, A. Mees, K. Judd and G. Froyland, *Determining the minimum embedding dimension of input–output time series data*, Int. J. Bif. Chaos, **8** (7), 1491–1504 (1998).

[11] David M. Walker, Reggie Brown, and Nicholas B. Tufillaro, *Constructing transportable behavioral models for nonlinear electronic devices*, Phys. Letts A **255** (4-6), 236-242, 1999.

[12] J. S. Lee and L. E. Miller, CDMA Systems Engineering Handbook, Artech House, Boston 1998.

[13] B. Murphy, *Diode and transistor self-analoques for circuit analysis*, The Bell System Technical Journal, 487-502, April 1968; E. Angelo, J. Logan, and K. Sussman, *The separation technique: A method for simulating transistors to aid integrated circuit design*, IEEE Trans. on Computers **C-17** (2), 113-116 (1968); H. Gummel and B. Murphy, *Circuit analysis by quasi-analog computation*, Proc. IEEE, 1758-1760 (1967).

[14] J. King, Matlab for Engineers, Addison-Wesley, San Francisco 1998.

[15] David M. Walker and Nicholas B. Tufillaro, *Radial basis models for feedback systems with fading memory* (preprint).

[16] Kevin Judd and Alistair Iain Mees, *On selecting models for nonlinear time series*. Physica D **82**, 426–444, 1995.